THE JOURNAL OF BIOLOGICAL CHEMISTRY VOL. 291, NO. 36, pp. 19079–19091, September 2, 2016


# Opposing Functions of the N-terminal Acetyltransferases Naa50 and NatA in Sister-chromatid Cohesion*

Received for publication, May 11, 2016, and in revised form, July 12, 2016 Published, JBC Papers in Press, July 15, 2016, DOI 10.1074/jbc.M116.737585

**Ziye Rong[‡], Zhuqing Ouyang[‡], Robert S. Magin[§], Ronen Marmorstein[§], and Hongtao Yu[‡1]**

*From the [‡]Howard Hughes Medical Institute, Department of Pharmacology, University of Texas Southwestern Medical Center, Dallas, Texas 75390 and [§]Department of Biochemistry and Biophysics, Abramson Family Cancer Research Institute, Perelman School of Medicine, University of Pennsylvania, Philadelphia, Pennsylvania 19104*

**During the cell cycle, sister-chromatid cohesion tethers sister chromatids together from S phase to the metaphase-anaphase transition and ensures accurate segregation of chromatids into daughter cells. N-terminal acetylation is one of the most prevalent protein covalent modifications in eukaryotes and is mediated by a family of N-terminal acetyltransferases (NAT). Naa50 (also called San) has previously been shown to play a role in sister-chromatid cohesion in metazoans. The mechanism by which Naa50 contributes to cohesion is not understood however. Here, we show that depletion of Naa50 in HeLa cells weakens the interaction between cohesin and its positive regulator sororin and causes cohesion defects in S phase, consistent with a role of Naa50 in cohesion establishment. Strikingly, co-depletion of NatA, a heterodimeric NAT complex that physically interacts with Naa50, rescues the sister-chromatid cohesion defects and the resulting mitotic arrest caused by Naa50 depletion, indicating that NatA and Naa50 play antagonistic roles in cohesion. Purified recombinant NatA and Naa50 do not affect each other's NAT activity *in vitro*. Because NatA and Naa50 exhibit distinct substrate specificity, we propose that they modify different effectors and regulate sister-chromatid cohesion in opposing ways.**

Proper chromosome segregation is essential for the correct transmission of genetic information (1). Errors during this process cause aneuploidy, which is linked to tumorigenesis and other human diseases (2–4). Sister-chromatid cohesion tethers sister chromatids from S phase to the metaphase-anaphase transition and ensures accurate alignment and segregation of chromosomes (5–7).

Timely establishment and dissolution of sister-chromatid cohesion are mediated by the cohesin complex and a set of regulatory proteins (6–9). In human cells, cohesin is composed of four core subunits, Smc1, Smc3, Scc1, and SA1/2. In telophase, cohesin is loaded onto chromosomes by the cohesin loader Scc2-Scc4 in a reaction that requires the ATPase activity of cohesin (10–13). The chromosome-bound cohesin remains dynamic in $G_1$ and can be released by the cohesin-releasing factors Wapl and Pds5 (14, 15). During DNA replication in S phase, Smc3 is acetylated on two conserved lysine residues by the acetyltransferase Esco1/2 (16–19). Smc3 acetylation enables the binding of sororin to cohesin through Pds5 (20–22). Sororin antagonizes the cohesin-releasing activity of Wapl-Pds5 and stabilizes cohesin on chromosomes, thus promoting sister-chromatid cohesion. In prophase, cohesin and sororin on chromosome arms are phosphorylated by Plk1 (polo-like kinase 1), Cdk1 (cyclin-dependent kinase 1), and other mitotic kinases and removed by Wapl-Pds5 (22–27). The centromeric cohesin is bound and protected by the Sgo1-PP2A complex (28–33). At the metaphase-anaphase transition, separase is activated and cleaves Scc1 to allow the separation of sister chromatids.

N-terminal acetylation is one of the most common covalent modifications of eukaryotic proteins (34). In human cells, the majority (around 85%) of proteins are N-terminally acetylated. N-terminal acetylation is catalyzed by a family of N-terminal acetyltransferases (NATs)[2] and occurs co-translationally on ribosomes (34). Genetic studies in *Drosophila* had initially revealed the role of the NAT separation anxiety protein (San; also called Naa50 or NatE) in sister-chromatid cohesion (35). Mutation of Naa50 disrupted sister-chromatid cohesion and caused premature sister-chromatid separation and mitotic arrest. A subsequent study showed that this function of Naa50 was conserved in humans, as depletion of Naa50 in HeLa cells by RNA interference (RNAi) caused phenotypes consistent with cohesion defects, including premature separation of sister chromatids and mitotic arrest (36). Deletion of Nat5, the closest homologue of Naa50 in *Saccharomyces cerevisiae*, did not cause overt phenotypes however (37). Therefore, Naa50 is required for sister-chromatid cohesion in metazoans but not in the budding yeast.

As a NAT, Naa50 prefers to acetylate the N terminus of proteins that retain the initiating methionine followed by a hydrophobic residue (34). This substrate specificity of Naa50 is consistent with structural studies, which show that the active site of Naa50 is ideally suited to accommodate the $\alpha$-amino group of a

* This work was supported by the Welch Foundation (I-1441; to H. Y.) and the Cancer Prevention and Research Institute of Texas (RP110465-P3 and RP120717-P2; to H. Y.). The authors declare that they have no conflicts of interest with the contents of this article.

[1] An Investigator with the Howard Hughes Medical Institute. To whom correspondence should be addressed. E-mail: hongtao.yu@utsouthwestern.edu.

[2] The abbreviations used are: NAT, N-terminal acetyltransferase; San, separation anxiety protein; Esco1/2, establishment of sister-chromatid cohesion 1/2; FISH, fluorescence *in situ* hybridization; FRAP, fluorescence recovery after photobleaching; Pds5, precocious dissociation of sister chromatids 5; PP2A, protein phosphatase 2A; SA1/2, stromal antigen 1/2; Scc1–4, sister chromatid cohesion 1–4; Sgo1, shugoshin 1; Smc1/3, structural maintenance of chromosomes 1/3; Wapl, winged apart like; IP, immunoprecipitate; MetAP, methionine amino peptidase; K-less, lysine-less.

methionine (38). In organisms from yeasts to humans, Naa50 interacts with the NatA complex, which consists the catalytic subunit Naa10 and the scaffolding subunit Naa15 (34, 36, 37). Unlike depletion of Naa50, depletion of NatA subunits does not cause apparent sister-chromatid cohesion defects (36), suggesting that Naa50 does not need to be in the Naa50-NatA complex to perform its cohesion functions. In addition to its NAT activity, Naa50 has been reported to harbor lysine acetyltransferase activity (39) and to undergo autoacetylation at lysine residues (36). Naa50 has also been reported to acetylate Lys-256 of tubulin to regulate microtubule dynamics (40). However, the ability of NATs to acetylate lysine residues has recently been called into question (41).

In this study we further explored the mechanism by which Naa50 regulates sister-chromatid cohesion. We first confirmed the requirement of the catalytic activity of Naa50 in sister-chromatid cohesion. Depletion of Naa50 in HeLa cells by RNAi caused cohesion defects in interphase. The cohesion defects caused by Naa50 depletion could be rescued by co-depletion of Wapl, suggesting that Naa50 promoted cohesion through antagonizing Wapl. Consistent with this notion, depletion of Naa50 weakened the binding of Pds5 and sororin to cohesin. Interestingly, depletion of either NatA subunit, Naa10 or Naa15, rescued the cohesion defect of Naa50-depleted cells. Recombinant Naa50 and NatA do not regulate each other's NAT activities *in vitro*. Our results suggest that Naa50 and NatA play opposing roles in sister-chromatid cohesion by acetylating different sets of substrates.

## Results

*Naa50 Promotes Sister-chromatid Cohesion through Catalytic and Non-catalytic Mechanisms*—A previous study showed that the Naa50 Y124F mutant, which had reduced acetyltransferase activities, did not rescue the sister-chromatid cohesion defects of human cells depleted of Naa50 by RNAi as efficiently as Naa50 wild type (WT) (36). This finding clearly demonstrated the involvement of the acetyltransferase activities of Naa50 in sister-chromatid cohesion. On the other hand, Naa50 Y124F was only partially defective in acetyltransferase activities (36). It was thus unclear whether partial rescue of Naa50 RNAi phenotypes by Naa50 Y124F was due to its partial activity or because of non-catalytic functions of Naa50. To distinguish between these two possibilities, we made the Naa50 F27A mutant and examined its cellular phenotypes.

Naa50 Phe-27 is highly conserved during evolution. The crystal structure of Naa50 bound to a peptide substrate, and CoA reveals that Phe-27 makes direct contacts with the N-terminal methionine (Fig. 1*A*) (38). The F27A mutation completely abolishes the NAT activity of Naa50 toward a peptide substrate with the sequence of MLGP (38). We first tested whether the F27A mutation also abolished the autoacetylation activity of Naa50. We performed *in vitro* acetylation assays by incubating recombinant GST-Naa50 WT or F27A with [$^{14}$C]acetyl-CoA (Fig. 1*B*). As expected, Naa50 WT underwent autoacetylation. The F27A mutation abolished this autoacetylation, indicating that Naa50 F27A lacked acetyltransferase activity. Naa50 has been shown to undergo autoacetylation at lysine residues (36). Our assay cannot distinguish whether GST-Naa50 undergoes autoacetylation at its own N terminus or at lysine residues. Regardless, even if Naa50 could indeed acetylate lysines, the Naa50 F27A mutant does not have detectable NAT or lysine acetyltransferase activities.

Depletion of Naa50 in human cells causes defects of sister-chromatid cohesion, premature sister-chromatid separation, and subsequent mitotic arrest dependent on the spindle checkpoint (36). We first confirmed that Naa50 depletion indeed caused mitotic arrest in both 293FT and HeLa cells (Fig. 1, *C–H*). A large percentage of mitotic 293FT cells depleted of Naa50 had separated sister chromatids (Fig. 1*E*). We next tested whether the catalytically inactive Naa50 F27A could rescue the mitotic arrest phenotype caused by Naa50 depletion. When expressed at similar levels (Fig. 1*F*), Naa50 F27A was less efficient than Naa50 WT in rescuing the mitotic arrest caused by Naa50 depletion (Fig. 1, *G* and *H*), confirming that the acetyltransferase activities of Naa50 were required for sister-chromatid cohesion. Interestingly, Naa50 F27A reduced the mitotic arrest caused by Naa50 depletion to some extent. This partial rescue by a catalytically inactive Naa50 mutant suggested that Naa50 might have non-catalytic roles in sister-chromatid cohesion.

*Naa50 Depletion Does Not Affect Cohesin Loading and Dynamics in Interphase*—Cohesion defects could be caused by defects in cohesion loading at telophase, cohesion establishment in S phase, or cohesion maintenance in early mitosis. We first examined whether Naa50 was required for cohesin loading in telophase. HeLa Tet-On cells were transfected with GFP-SA2 plasmids then either mock-transfected or transfected with siNaa50 and enriched at telophase with a thymidine-arrest-release protocol and fixed and stained (Fig. 2, *A–C*). Tubulin staining was used to identify telophase cells, which had a prominent central spindle. Depletion of Naa50 did not substantially reduce the percentage of telophase cells with chromatin-bound GFP-SA2. About 30% of telophase cells in both groups exhibited strong GFP-SA2 staining on chromatin. The subgroup of Naa50 RNAi cells that was able to progress to telophase presumably contained residual Naa50 during that cell cycle and was expected to undergo mitotic arrest in the ensuing cell cycle. Therefore, consistent with an earlier report (36), Naa50 appears to be dispensable for cohesin loading.

To further validate that cohesin was properly loaded in Naa50 RNAi cells, we examined the cohesin dynamics on interphase chromatin using fluorescence recovery after photobleaching (FRAP). HeLa Tet-On cells stably expressing Smc1-GFP were either mock-transfected or transfected with siNaa50, arrested at the $G_1$/S boundary with thymidine, and subjected to FRAP analysis (Fig. 2, *D–F*). Naa50 depletion did not alter the half-life or plateau of Smc1-GFP recovery on interphase chromatin. Thus, Naa50 does not regulate the dynamics of bulk cohesin in interphase nucleus. By inference, these results suggest that cohesin is intact and loaded properly on chromosomes before DNA replication in Naa50-deficient cells.

*Naa50 Is Required for the Establishment of Sister-chromatid Cohesion in S Phase*—We next tested whether Naa50 was required for cohesion establishment in S phase. HeLa

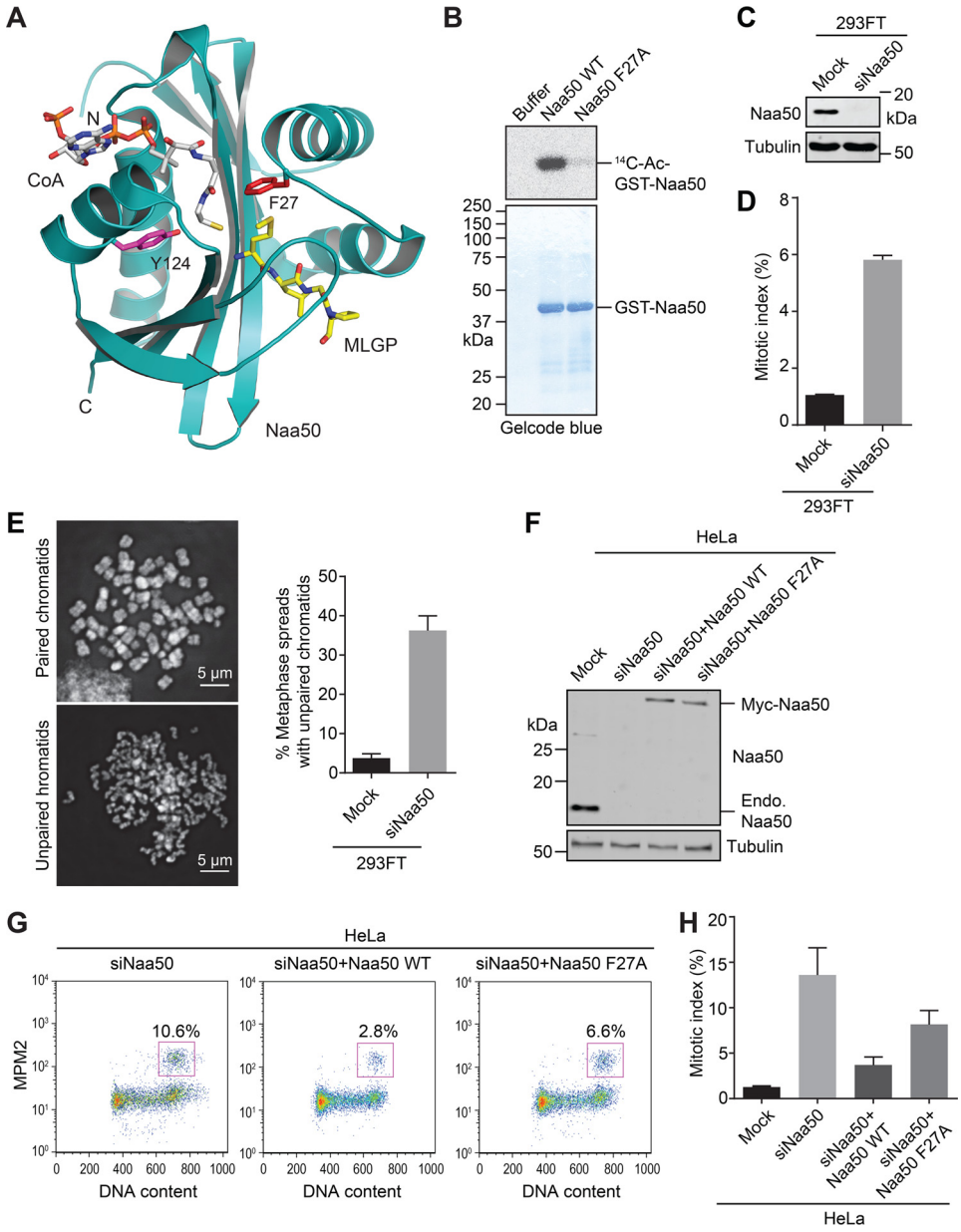


FIGURE 1. **Naa50 has both catalytic and non-catalytic roles in sister-chromatid cohesion.** *A*, ribbon diagram of the structure of human Naa50 with the bound CoA and the MGLP peptide substrate shown in *sticks*. Two residues close to the active site, Phe-27 and Tyr-124, are also shown in *sticks*. *B*, autoacetylation of GST-Naa50 wild type (*WT*) and F27A in the presence of [$^{14}$C]acetyl-CoA. The reaction mixtures were separated on SDS-PAGE, stained with GelCode blue (*bottom panel*), and subjected to autoradiography with phosphorimaging (*top panel*). Representative image of more than three independent experiments is shown. *C*, immunoblots of lysates of 293FT cells transfected with the indicated siRNAs. Tubulin was blotted as the loading control. Representative image of two independent experiments is shown. *D*, quantification of the mitotic indices (defined as the percentage of MPM2-positive 4N cells) of cells in *C*. Results are the mean ± range, $n = 2$ independent experiments. *E*, representative metaphase spread images of 293FT cells transfected with the indicated siRNAs and treated with nocodazole for 3 h. Metaphase spreads with mostly paired chromatids (*top*) or with separated chromatids (*bottom*) are shown. The percentages of metaphase spreads with mostly separated chromatids are quantified and shown on the *right*. Results are the mean ± range, $n = 2$ independent experiments. *F*, immunoblots of lysates of HeLa Tet-On cells transfected with the indicated siRNA and plasmids. Tubulin was blotted as the loading control. The positions of the endogenous Naa50 and Myc-Naa50 proteins are labeled. Representative images of four independent experiments are shown. *G*, representative FACS graphs of cells in *F*. Mitotic cells (MPM2-positive 4N cells) are *boxed* and quantified. *H*, quantification of the mitotic indices (defined as the percentage of MPM2-positive 4N cells) of cells in *F*. Results are the mean ± range, $n = 2$ independent experiments.

Tet-On cells were depleted of Naa50 and synchronized in S phase with the thymidine-arrest-release protocol and subjected to fluorescence *in situ* hybridization (FISH) analysis with a probe that recognized the q arm of chromosome 21 (Fig. 3*A*). The distances between paired FISH dots were measured for multiple cells in both the mock-transfected and siNaa50-transfected groups (Fig. 3*B*). Strikingly, depletion of Naa50 significantly increased the distances of paired FISH signals, indicative of cohesion defects. This result strongly suggests that Naa50 is required for cohesion establishment in S phase.

We next performed metaphase spreads on mitotic Naa50 RNAi cells (Fig. 3, *C* and *D*). About 50% the mitotic cells depleted of Naa50 had separated sister chromatids, whereas the vast majority of mock-transfected cells contained paired sister chromatids. Thus, the interphase cohesion defects caused by

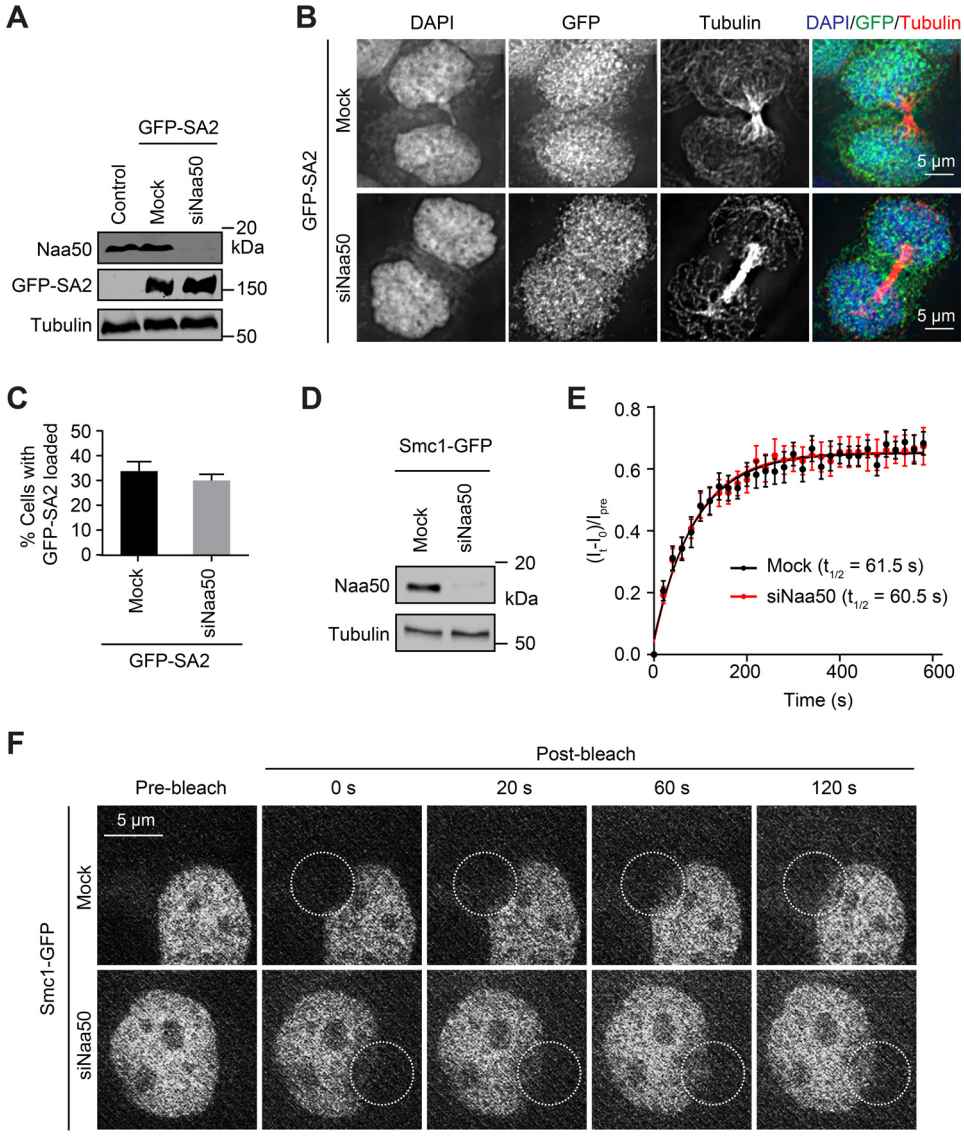


FIGURE 2. **Naa50 is dispensable for cohesin loading and dynamics.** *A*, immunoblots of HeLa Tet-On cells transfected with the indicated siRNA and plasmids. A representative image of three independent experiments is shown. *B*, immunofluorescence staining of cells in *A* that had been synchronized at telophase. DAPI, GFP, and tubulin staining was pseudo-colored *blue*, *green*, and *red*, respectively, in the merged images. *C*, quantification of the percentage of telophase cells with positive GFP-SA2 staining on chromatin. Results are the mean ± range, $n = 2$ independent experiments with 40 cells counted for each group in each experiment. *D*, immunoblots of HeLa Tet-On cells stably expressing Smc1-GFP that had been mock-transfected or transfected with siNaa50. A representative image of three independent experiments is shown. *E*, quantification of relative fluorescent signals during FRAP. Data were collected from 10 cells for each group in three independent experiments. *Error bars*, S.E. The $t_{1/2}$ values are listed below. *F*, representative Smc1-GFP images of cells in *D* before and at different times after photobleaching. The bleached areas are marked by *dashed circles*.

Naa50 depletion lead to premature sister-chromatid separation and mitotic arrest.

A major mechanism of cohesion establishment is through antagonizing the cohesin-releasing activity of Wapl (9). To test whether Naa50 also promoted cohesion through antagonizing Wapl, we co-depleted Naa50 and Wapl from HeLa Tet-On cells and examined their cohesion status by metaphase spreads. Co-depletion of Wapl rescued the premature sister-chromatid separation and the subsequent mitotic arrest seen in Naa50-depleted cells (Fig. 3, *C–E*). These results suggest that Naa50 regulates sister-chromatid cohesion through antagonizing Wapl.

*Naa50 Promotes Binding of Sororin to Cohesin*—During S phase, acetylation of Smc3 at two conserved lysine residues by Esco1 and Esco2 antagonizes Wapl to promote the establishment of sister-chromatid cohesion (16–18). We tested whether Naa50 regulated cohesion establishment through Smc3 acetylation (Fig. 4*A*). HeLa Tet-On cells were depleted of Naa50, synchronized in S phase, and fractionated into cytosolic and nuclear fractions. Virtually all Smc3 was found in the nuclear fraction, whereas Naa50 was predominantly in the cytosolic fraction. As expected, depletion of Esco1 and Esco2 greatly reduced Smc3 acetylation in S phase. In contrast, Naa50 depletion did not affect the level of Smc3 acetylation. These results indicate that Naa50 antagonizes Wapl and regulates sister-chromatid cohesion through a mechanism that is independent of Smc3 acetylation.

Smc3 acetylation enables the binding of Pds5 and sororin to cohesin (22). Sororin antagonizes Wapl in part through directly competing for interactions with cohesin and Pds5 (15, 22).

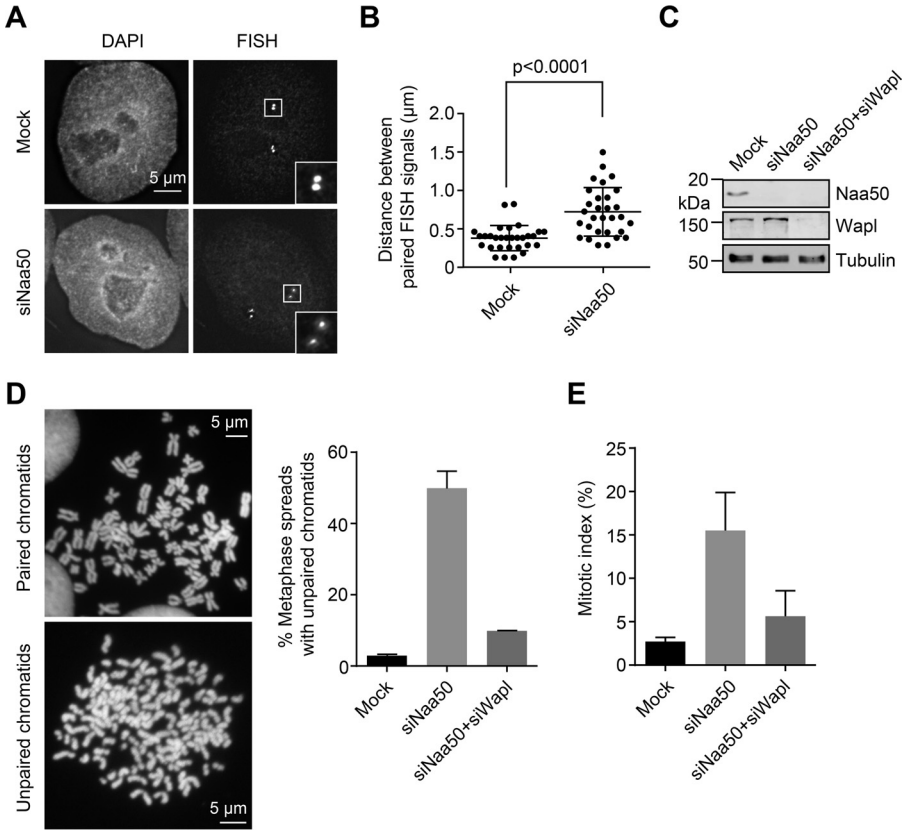


FIGURE 3. **Naa50 promotes the establishment of sister-chromatid cohesion through antagonizing Wapl.** *A*, representative images of mock or siNaa50 transfected HeLa Tet-On cells synchronized at S phase and stained with DAPI and FISH probes. The *boxed* regions are magnified in the *inset*. *B*, quantification of distances between paired FISH signals of cells in *A*. Mean ± S.D. is shown. Data were collected in two independent experiments. *p* value was calculated with Student's *t* test. *C*, immunoblots of lysates of HeLa Tet-On cells transfected with the indicated siRNAs. Tubulin was blotted as the loading control. A representative image of eight independent experiments is shown. *D*, representative metaphase spread images of HeLa Tet-On cells transfected with the indicated siRNAs and treated with nocodazole for 3 h. Metaphase spreads with mostly paired chromatids (*top*) or with separated chromatids (*bottom*) are shown. The percentages of metaphase spreads with mostly separated chromatids are quantified and shown on the *right*. Results are the mean ± range, $n = 2$ independent experiments. *E*, quantification of mitotic indices of HeLa Tet-On cells transfected with the indicated siRNAs. Results are the mean ± S.D., $n = 3$ independent experiments.

Next, we investigated whether Naa50 regulated the binding of sororin to cohesin. HeLa Tet-On cells were depleted of Naa50 and synchronized in late S/$G_2$ phase by the thymidine-arrest-release method (Fig. 4*B*). Cell lysates were subjected to immunoprecipitation with beads coupled to anti-sororin or anti-Smc1 antibodies. Depletion of Naa50 greatly reduced the amount of Smc1 and Scc1 in the anti-sororin immunoprecipitate (*IP*; Fig. 4*C*). Naa50 depletion also reduced the amount of sororin in the anti-Smc1 IP without affecting the amount of Scc1 in this IP. Naa50 depletion only slightly weakened the association of Pds5 binding to cohesin or sororin. Thus, Naa50 is required for the proper association of sororin to cohesin without compromising the integrity of the cohesin complex. This defect suffices to explain the cohesion establishment defects of Naa50 depletion.

In prophase, Sgo1-PP2A binds to and protects centromeric cohesin from mitotic kinases and Wapl-dependent release (33). Although defective sororin binding and interphase cohesion defects can explain the premature sister-chromatid separation phenotypes of Naa50 RNAi cells, it remained formally possible that Naa50 might be additionally involved in centromeric cohesion protection. We thus directly examined whether Naa50 depletion affected the Sgo1-dependent cohesion maintenance mechanism in mitosis. HeLa Tet-On cells stably expressing Myc-Sgo1 were cultured in the absence or presence of doxycycline and depleted of Naa50 and synchronized in mitosis using the thymidine-arrest-release protocol. Mitotic cells were collected with shake-off. Lysates were subjected to anti-Myc IP. Naa50 depletion did not reduce the amount of Smc1 present in the anti-Myc-Sgo1 IP (Fig. 4*D*). This result along with the previously reported finding that Naa50 depletion does not affect the kinetochore localization of Sgo1 (36) suggests that Naa50 is not involved in Sgo1-dependent centromeric cohesion protection.

*Scc1 and Sororin Do Not Appear to Be Functional Naa50 Substrates*—We took a candidate approach to investigate the mechanisms by which Naa50 enhanced the interaction between sororin and cohesin. Because Naa50 has been reported to harbor both NAT and lysine acetyltransferase activities, we considered potential substrates for both activities. The N-terminally tagged human Scc1 failed to rescue the mitotic arrest phenotype caused by Scc1 depletion, whereas the C-terminally tagged Scc1 could,[3] indicating that tagging Scc1 at its N termi-

[3] S. Kim and H. Yu, unpublished results.

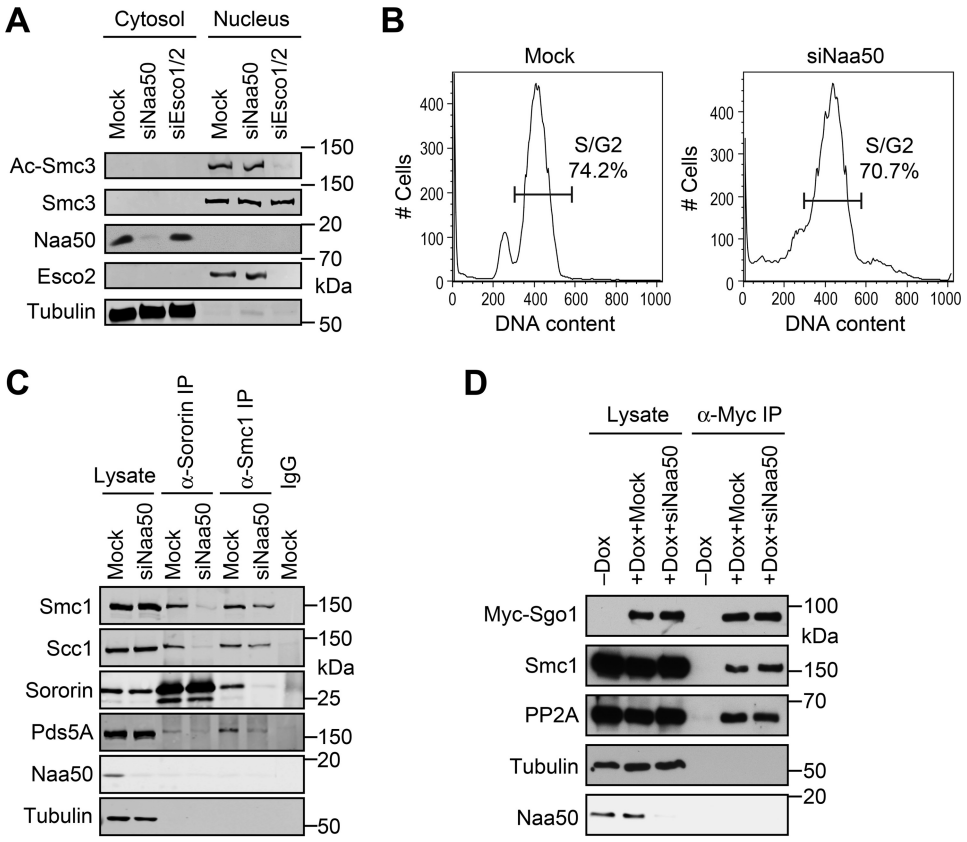


FIGURE 4. **Naa50 promotes sororin binding to cohesin without affecting Smc3 acetylation.** *A*, immunoblots of the cytosolic and nuclear fractions of HeLa Tet-On cells transfected with the indicated siRNAs. Representative image of three independent experiments is shown. *B*, FACS profiles of mock or siNaa50 transfected HeLa Tet-On cells synchronized at late S/$G_2$. The percentages of S/G2 cells are quantified. *C*, immunoblots of lysates, IgG IP, anti-sororin IP, and anti-Smc1 IP of cells in *B*. A representative image of >10 independent experiments is shown. *D*, HeLa Tet-On cells stably expressing Myc-Sgo1 were mock- or siNaa50-transfected and synchronized in mitosis. Mitotic cells were collected by shake-off. The total cell lysates and anti-Myc IP were blotted with the indicated antibodies. A representative image of five independent experiments is shown.

nus rendered it inactive. Furthermore, the N-terminal region of Scc1 matches the Naa50 consensus and is highly conserved in most species with the exception of *S. cerevisiae* where the closest homolog of Naa50 is not required for cohesion (Fig. 5*A*). Moreover, the N-terminal tagging of all other cohesin subunits and regulators, including Smc1, Smc3, SA2, Pds5B, Wapl, and sororin, produces functional fusion proteins (15, 22, 42, 43), suggesting that an acetylated natural N terminus is not critical for their functions. Finally, proteomic studies revealed that the N terminus of human Scc1 could be acetylated (44). We thus tested whether Scc1 was a potential NAT substrate of Naa50.

We made an antibody against the Nα-acetylated Scc1N peptide. This antibody preferably recognized Scc1N-GST that had been incubated with Naa50 and acetyl-CoA (Fig. 5*B*). This result indicates that Naa50 can acetylate the N terminus of Scc1 *in vitro*. This antibody also recognized a band in the cytosolic fraction of HeLa cell lysates whose intensity was reduced by Naa50 RNAi (Fig. 5*C*). Unfortunately, the intensity of this band was not reduced by Scc1 RNAi, indicating that our anti-Ac-Scc1N antibody cross-reacted with an N-terminally acetylated cytosolic Naa50 substrate. All authentic Scc1 protein was present in the nuclear fraction. The anti-Ac-Scc1N antibody detected weak bands in the nuclear fraction, which were absent in the Scc1 RNAi sample. The intensities of these weak bands were not altered by Naa50 RNAi however. In repeated attempts, we failed to detect N-terminally acetylated peptides of endogenous Scc1 immunopurified from HeLa cells, although we could readily detect unmodified N-terminal peptides of Scc1. Thus, the N terminus of Scc1 is not strongly acetylated, and any weak N-terminal acetylation of Scc1 does not require Naa50.

For the potential lysine acetyltransferase substrate of Naa50, we focused on sororin, as it bound to cohesin more weakly in Naa50-depleted cells. A recombinant C-terminal sororin fragment was indeed acetylated by Naa50 *in vitro* (Fig. 5*D*). Mass spectrometry analysis identified two acetylated lysines, Lys-187 and Lys-197, in this region of sororin (Fig. 5*E*). Mutation of these two lysines to arginine, however, did not reduce the Naa50-dependent acetylation of sororin, indicating that there were additional Naa50 acetylation sites either at the N terminus or at additional lysines. We thus created a lysine-less (K-less) mutant of sororin (with all lysines mutated to arginine). The expression level of sororin K-less protein was higher than that of sororin WT (Fig. 5*F*), consistent with sororin being a short-lived ubiquitinated protein. Expression of Myc-sororin K-less rescued the mitotic arrest caused by sororin depletion as efficiently as did the WT (Fig. 5*G*). Even when we reduced the amount of sororin K-less plasmid to make its expression comparable to WT (Fig. 5*H*), there was still no difference in the efficiency of rescue between the WT and K-less samples

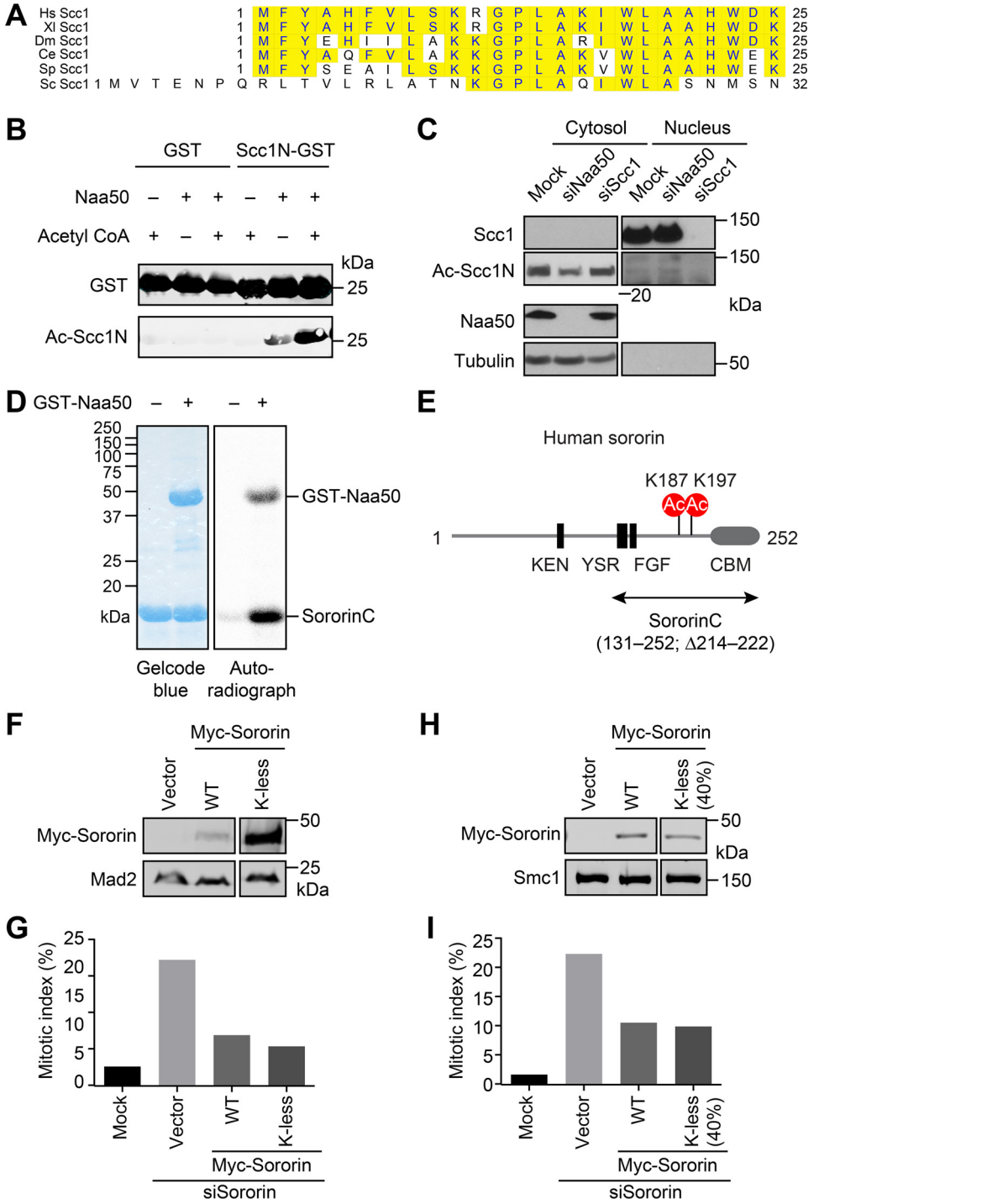


FIGURE 5. **Scc1 and sororin are not functionally relevant substrates of Naa50 in cohesion.** *A*, sequence alignment of the N-terminal region of Scc1 proteins from different species. *Hs*, *Homo sapiens*; *Xl*, *Xenopus laevis*; *Dm*, *Drosophila melanogaster*; *Ce*, *Caenorhabditis elegans*; *Sp*, *Schizosaccharomyces pombe*; *Sc*, *Sacchromyces cerevisiae*. *B*, immunoblots of recombinant GST or Scc1N-GST proteins that had been incubated in the presence or absence of Naa50 or acetyl-CoA. Representative image of two independent experiments is shown. *C*, immunoblots of cytosolic and nuclear fractions of HeLa Tet-On cells transfected with the indicated siRNAs. Representative image of two independent experiments is shown. *D*, recombinant purified sororinC protein (residues 131–252 with the basic region 214–222 deleted) was incubated with [$^{14}$C]acetyl-CoA in the presence or absence of GST-Naa50. The reaction mixtures were separated on SDS-PAGE, stained with GelCode blue (*right panel*) and subjected to autoradiography with phosphorimaging (*left panel*). *E*, schematic drawing of human sororin with its domains and motifs shown. The boundary of sororinC is indicated. The two acetylated lysines are also labeled. *F* and *H*, immunoblots of lysates HeLa Tet-On cells depleted of sororin and transiently transfected with Myc-sororin wild type (*WT*) or the lysine-less (*K-less*) mutant. Mad2 and Smc1 were used as loading controls. *G* and *I*, quantification of the mitotic indices of cells in *F* and *H*, respectively, by FACS.

(Fig. 5*I*). These results indicate that lysine acetylation is not absolutely required for the function of sororin. We cannot exclude the possibility that lysine acetylation of sororin promotes sister-chromatid cohesion through antagonizing other forms of lysine modification, which are also disrupted in the K-less mutant. Regardless, we cannot obtain definitive evidence to implicate either Scc1 or sororin as functional Naa50 substrates.

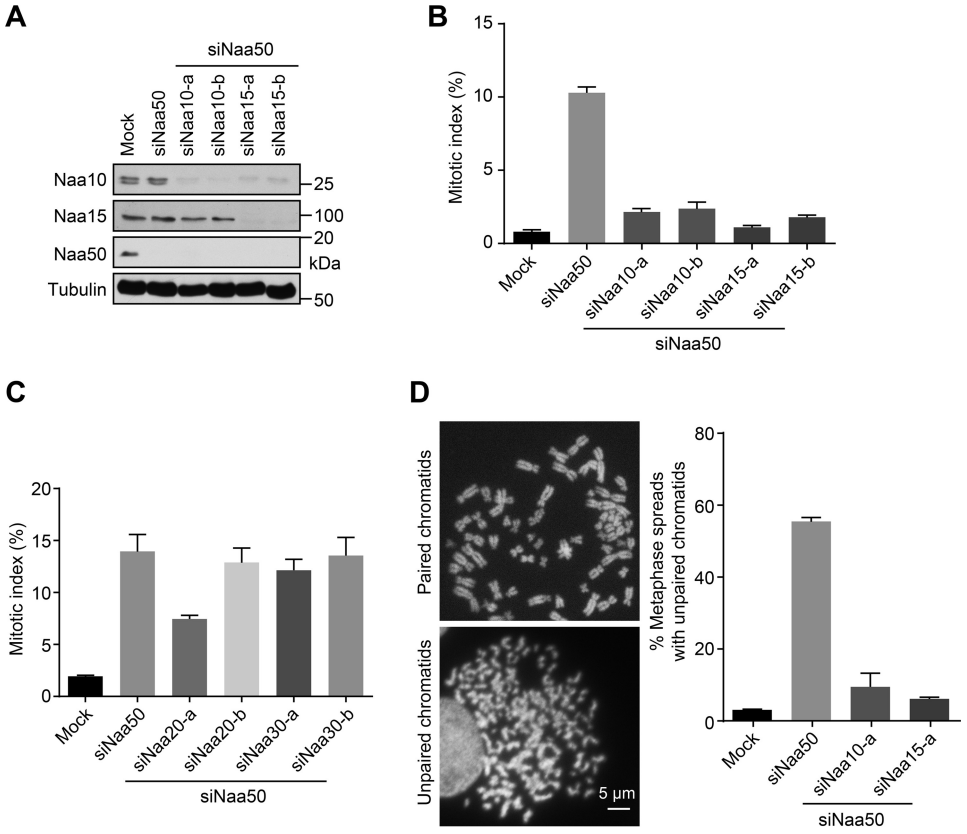


FIGURE 6. **Naa50 opposes NatA in sister-chromatid cohesion.** *A*, immunoblots of HeLa Tet-On cells transfected with the indicated siRNAs. A representative image of >10 independent experiments is shown. *B*, quantification of mitotic indices of cells in *A* as determined by FACS. Results are the mean ± range, $n = 2$ independent experiments. *C*, quantification of mitotic indices of HeLa Tet-On cells transfected with the indicated siRNAs by FACS. Results are the mean ± range, $n = 2$ independent experiments. *D*, representative metaphase spread images of HeLa Tet-On cells transfected with the indicated siRNAs and treated with nocodazole for 3 h. Metaphase spreads with mostly paired chromatids (*top*) or with separated chromatids (*bottom*) are shown. The percentages of metaphase spreads with mostly separated chromatids are quantified and shown on the *right*. Results are the mean ± range, $n = 2$ independent experiments.

*NatA Depletion Rescues Cohesion Defects Caused by Naa50 Depletion*—Because we could not identify direct Naa50 substrates among cohesin subunits and regulators, we examined the possibility that Naa50 indirectly regulated sister-chromatid cohesion. Naa50 is known to associate with NatA, which consists of the catalytic subunit Naa10 and the scaffolding subunit Naa15. NatA has a broader substrate specificity than Naa50 and acetylates small polar or hydrophobic residues at the N termini of proteins that are exposed after the cleavage of the initiating methionine by methionine amino peptidases (MetAP1/2) (34, 45). A previous study has already demonstrated that NatA is not required for sister-chromatid cohesion in human cells (36). We tested whether NatA regulated the function of Naa50 in cohesion by performing a double depletion experiment. Strikingly, depletion of either NatA subunits, Naa10 or Naa15, rescued the mitotic arrest phenotype caused by Naa50 depletion (Fig. 6, *A* and *B*). Two siRNAs against each NatA subunits produced similar results. Depletion of Naa15 also reduced the protein level of Naa10, presumably because that Naa10 required Naa15 for proper folding or stability. As a control, depletion of Naa20 (the catalytic subunit of NatB) or Naa30 (the catalytic subunit of NatC) did not efficiently rescue the mitotic arrest phenotype of Naa50 RNAi cells (Fig. 6*C*). As expected, depletion of Naa10 or Naa15 recued the premature sister-chromatid separation seen in mitotic Naa50 RNAi cells (Fig. 6*D*). These results suggest that Naa50 might promote sister-chromatid cohesion through opposing the function of NatA.

*Naa50 and NatA Do Not Regulate each Other in Vitro*—We next tested whether Naa50 blocked the activity of NatA and vice versa *in vitro* (Fig. 7, *A* and *B*). Recombinant Naa50 efficiently acetylated the peptide substrate with the sequence of MLGP (Fig. 7*B*) but did not acetylate the SASE peptide, consistent with its preference for an N-terminal methionine. Conversely, NatA only acetylated SASE but did not acetylate MLGP. The distinct specificities of Naa50 and NatA allowed us to test whether they regulated each other's activity in the Naa50-NatA complex. Naa50 when bound to NatA was still active in acetylating the MLGP peptide (Fig. 7*B*). The lower activity of the Naa50-NatA complex was likely due to the lower amount of Naa50 present in the complex, as compared with Naa50 alone (Fig. 6*A*; compare the *second* and *third lanes*). Likewise, NatA in the Naa50-NatA complex also retained activity against SASE (Fig. 7*B*). In this case the elevated activity of NatA in the complex was caused by the higher amount of Naa10, the catalytic subunit of NatA, in the Naa50-NatA complex (Fig. 7*A*; compare the *first* and *third lanes*). Therefore, Naa50 and NatA do not mutually inhibit the activity of each other *in vitro*. The antagonism between Naa50 and NatA in sister-chromatid cohesion is mediated by indirect mechanisms.

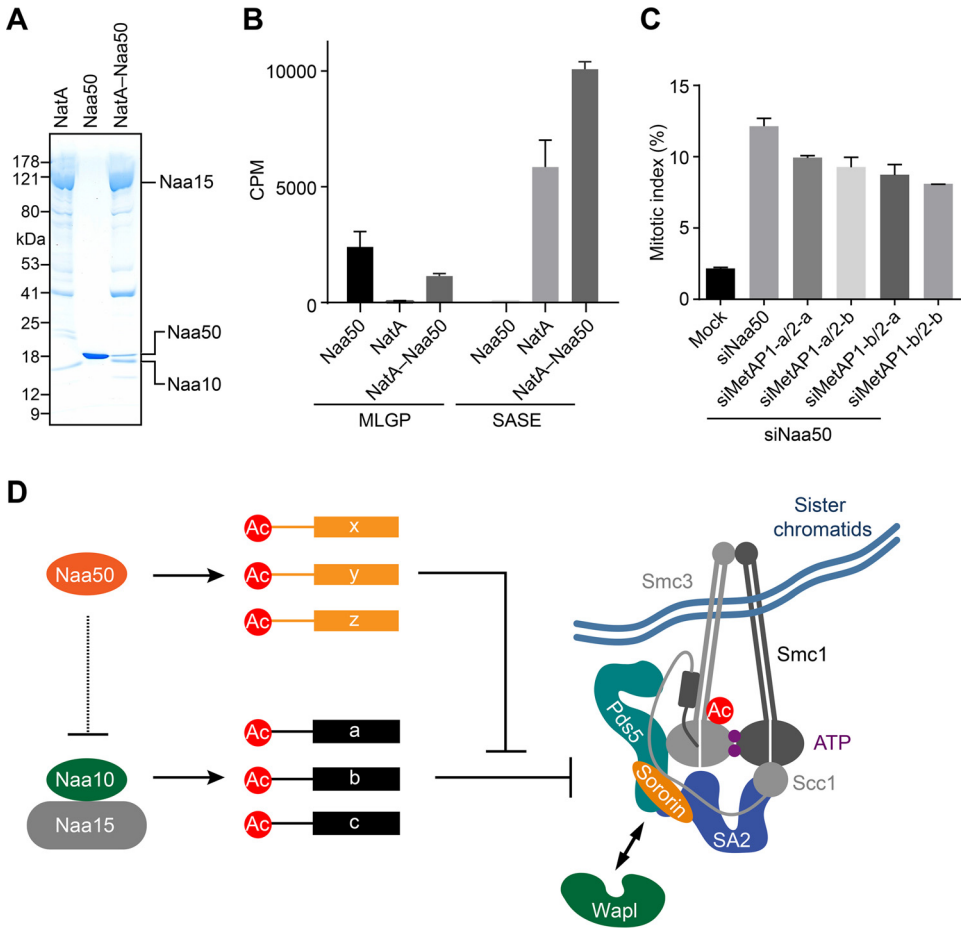


FIGURE 7. **Naa50 and NatA do not mutually regulate the activities of each other.** *A*, Coomassie stained gel of recombinant purified Naa50, NatA (the Naa10-Naa15 complex), and the Naa50-NatA complex. *B*, acetyltransferase activities of enzymes in *A* using the MLGP or SAGE peptides as substrates. Results are the mean ± S.D. of the reactions in triplicate. *C*, quantification of mitotic indices of HeLa Tet-On cells transfected with the indicated siRNAs by FACS. Results are the mean ± range, $n = 2$ independent experiments. *D*, model for the opposing roles of Naa50 and NatA in sister-chromatid cohesion. In this model Naa50 and NatA acetylate different sets of substrates. NatA-mediated acetylation weakens cohesion through modulating the cohesin-sororin interaction. Naa50-dependent acetylation counteracts this effect of NatA. Naa50 might also directly inhibit NatA during translation *in vivo*.

## Discussion

N-terminal acetylation is one of the most prevalent covalent modifications on proteins and occurs co-translationally on the majority of eukaryotic proteins. Recently, several prominent examples have established the functional importance of N-terminal acetylation in certain cases (46, 47). Furthermore, the NATs have been proposed to be potential molecular targets for anti-cancer therapies (34). In this study we have shown that two NATs, NatA and Naa50, have opposing roles in sister-chromatid cohesion.

Naa50-deficient cells exhibit defects in cohesion establishment in S phase and premature sister-chromatid separation in mitosis. These defects are caused by the weakened binding of the positive cohesion regulator, sororin, to cohesin. Interestingly, Naa50 depletion does not affect Smc3 acetylation by Esco1/2, the known mechanism for recruiting sororin to cohesin. Therefore, our findings suggest that an Smc3 acetylation-independent mechanism promotes sororin binding to cohesin and regulates cohesion establishment during S phase. Naa50-mediated acetylation is required for this yet-to-be-discovered mechanism. Although our extensive searches have failed to identify the relevant substrates of Naa50 in cohesion establishment, we have provided strong evidence to rule out the N terminus of Scc1 and the lysines of sororin as obligatory substrates of Naa50.

In organisms from yeast to man, Naa50 physically interacts with NatA but not other NATs. Surprisingly, depletion of NatA, but not NatB or NatC, rescues the cohesion defects caused by Naa50 depletion, suggesting that Naa50 promotes cohesion specifically through antagonizing NatA. Although Naa50 does not inhibit the activity of NatA *in vitro*, it remains possible that Naa50 might restrict the activity of NatA when both are bound to the ribosomes during protein translation *in vivo*. The direct binding of Naa50 to NatA might be important for its functional interference of NatA, a notion consistent with a non-catalytic role of Naa50 in cohesion. The identification of Naa50 mutants that cannot bind to NatA is required to test this possibility in human cells.

Naa50 prefers to acetylate the N terminus of proteins that retain the initiating methionine, whereas NatA is inactive against Naa50 substrates and can only acetylate proteins with the initiating methionine cleaved by MetAPs. A recent study showed that the acetylation of the initiating methionine of certain proteins by Naa50 blocks their processing by MetAPs and

subsequent acetylation of the second residue by NatA (48). A potential MetAP-dependent competition for the same set of substrates could explain the functional antagonism between Naa50 and NatA in sister-chromatid cohesion. If this hypothesis were true, inactivation of MetAPs would be expected to produce phenotypes similar to NatA inactivation. Unfortunately, unlike NatA depletion, depletion of both MetAP1/2 failed to rescue the cohesion defects and mitotic arrest caused by Naa50 depletion (Fig. 7*C*). This finding does not lend support to the hypothesis of MetAP-mediated substrate competition between Naa50 and NatA.

Taking all available evidence into account, we propose the following hypothesis to explain the functional antagonism between Naa50 and NatA in sister-chromatid cohesion (Fig. 7*D*). In this hypothesis, Naa50 and NatA acetylate different sets of substrates. NatA-mediated acetylation has a net negative effect on sister-chromatid cohesion. Naa50-dependent acetylation counteracts this inhibitory effect of NatA, thus indirectly promoting cohesion. Given the broad specificity of NATs, it is quite possible that Naa50 and NatA each have a large number of substrates instead of a handful of functional substrates. The collective effects of these acetylation events determine the status of sister-chromatid cohesion, with acetylation of each substrate having a small effect. Future studies that examine the N-terminal and lysine acetylation status at the proteome level in cells deficient for Naa50 or NatA or both are needed to test this hypothesis.

## Experimental Procedures

*Cell Culture and Cell Cycle Synchronization*—HeLa Tet-On (Invitrogen) cells were grown in Dulbecco's modified Eagle's medium (DMEM; Invitrogen) supplemented with 10% fetal bovine serum, 2 mM L-glutamine, and penicillin-streptomycin. For cell cycle synchronization, cells were arrested at $G_1$/S by the addition of 2 mM thymidine (Sigma) for 18 h. Cells synchronized at S, $G_2$, and late mitosis were collected at 4, 7, and 11 h after the release from the thymidine arrest, respectively. For mitotic arrest, cells released from the thymidine arrest for 8 h were further treated with 300 nM nocodazole (Sigma) for another 4 h and collected.

*Cellular Fractionation*—Cellular fractionation was performed as described by Mendez *et al.* (49). Briefly, cell pellet was resuspended in Buffer A (10 mM HEPES, pH 7.9, 10 mM KCl, 1.5 mM $MgCl_2$, 0.34 M Sucrose, 10% Glycerol, 0.1% Triton X-100, 1 mM DTT, and 1× protease inhibitor mixture (Roche Applied Science)). After an 8-min incubation on ice, the nuclear fraction was pelleted by centrifugation at 1300 × *g* for 5 min at 4 °C and resuspended in SDS sample buffer. The supernatant was collected as the cytoplasmic fraction.

*Plasmid and siRNA Transfection*—Cells were treated with the desired plasmids with the Effectene reagent (Qiagen) according to the manufacturer's protocols. Myc-Sgo1 and GFP-Smc1 stable cell lines were made by transfecting HeLa Tet-On cells with pTRE2 vectors encoding RNAi-resistant human Myc-Sgo1 and GFP-Smc1 and selected with hygromycin (Invitrogen). The surviving clones were picked and screened for the doxycycline-induced expression of Myc-Sgo1 or GFP-Smc1 using immunoblotting.

For RNAi experiments, HeLa Tet-On cells were transfected with siRNAs with Lipofectamine RNAiMax (Invitrogen) according to the manufacturer's protocols. The siRNA oligonucleotides used in this study are: Naa50 siRNA (5′-GCUACAAUGACAAGUUCUAdTdT-3′), Wapl siRNA (5′-CGGACUACCCUUAGCACAAdTdT-3′), Scc1 siRNA (5′-GGAAGAAGCATTTGCATTGdTdT-3′), Esco1 siRNA (Dharmacon ON-TARGETplus set of 4), Esco2 siRNA (Dharmacon ON-TARGETplus set of 4), Naa10 siRNAs (siGENOME D-009606-02, D-009606-03, Thermo Scientific), Naa15 siRNAs (siGENOME D-012847-01, D-012847-03, Thermo Scientific), Naa20 siRNAs (siGENOME D-008944-03, D-008944-04, Thermo Scientific), Naa30 siRNAs (siGENOME D-009961-01, D-009961-06, Thermo Scientific), MetAP1 siRNAs (siGENOME D-008693-01, D-008693-02, Dharmacon), MetAP2 siRNAs (siGENOME D-005943-06, D-005943-07, Dharmacon).

*Antibodies, Immunoprecipitation, and Immunoblotting*—The rabbit polyclonal antibody against human Naa50 was raised by Genemed Synthesis Inc. using $His_6$-tagged recombinant Naa50 as the antigen (36). The resulting crude serum was affinity-purified before use. The rabbit polyclonal antibody against N-terminal acetylated Scc1 (Ac-Scc1N) was raised in an in-house facility with a synthetic peptide (Ac-MFYAHFVLS) as the antigen. The resulting crude serum was affinity-purified before use. Rabbit polyclonal antibodies to enhanced GFP, human Sgo1, and human sororin were raised at Yenzym with recombinant proteins or protein fragments as antigens. The following antibodies were purchased from the indicated sources: Myc (Roche Applied Science 11667203001), Naa10 (Santa Cruz sc-373920), Naa15 (Santa Cruz sc-365931), Scc1 (Bethyl A300-080A), Smc1 (Bethyl A300-055A), Smc3, Ac-Smc3 (MBL PD040), Esco2 (Bethyl A301–689A), Tubulin (Sigma T9026), Pds5A (Bethyl A300-089A), and MPM-2 (Millipore 05-368).

For immunoprecipitation, anti-Smc1, anti-Myc, or affinity-purified anti-sororin antibodies were coupled to Affi-Prep Protein A beads (Bio-Rad) at a concentration of 1 mg/ml. Cells were lysed with the lysis buffer containing 25 mM Tris-HCl at pH 7.5, 75 mM NaCl, 5 mM $MgCl_2$, 5 mM NaF, 0.1% Nonidet P-40, 10 mM β-glycerophosphate, 0.5 μM okadaic acid, 0.3 mM $Na_3VO_4$, 1 mM DTT, 1× protease inhibitor mixture (Roche Applied Science), and 50 unit/ml Turbo-nuclease (Accelagen). The cell lysate was incubated on ice for 2 h and then at 37 °C for 10 min. The lysate was cleared by centrifugation at 13,200 *g* at 4 °C for 20 min. The supernatant was incubated with the desired antibody beads for 2 h at 4 °C. The beads were washed three times with the lysis buffer. The proteins bound to beads were dissolved in SDS sample buffer, separated by SDS-PAGE, and blotted with the appropriate antibodies. For immunoblotting, the purified antibodies were used at 1 μg/ml final concentration. The commercial antibodies were used at 1:500 or 1:1000 dilutions depending on the stock concentrations.

*Protein Expression and Purification*—The cDNAs encoding human Naa50 WT and F27A were cloned into the pGEX6p-1 vector to produce N-terminal GST fusion proteins. The cDNA encoding of the N-terminal peptide of human Scc1 (MFYAHFVLSKR) was also cloned into pGEX6p-1 to produce a C-terminal GST fusion protein. These vectors were transformed into the *Escherichia coli* strain BL21. Protein expression was

induced by the addition of isopropyl 1-thio-β-D-galactopyranoside (0.2 mM) at 16 °C for overnight. Recombinant Scc1N-GST and GST-Naa50 WT and F27A proteins were purified with the glutathione-Sepharose 4B resin (GE Healthcare).

*In Vitro Acetylation Assays*—For Naa50 lysine autoacetylation, 2 μg of GST-Naa50 proteins (WT or F27A) were incubated in the acetylation buffer (50 mM Tris-HCl, pH 7.5, 100 mM NaCl, and 10% glycerol) with 70 μM [$^{14}$C]acetyl-CoA (4 mCi/mmol; PerkinElmer Life Sciences, NEC313050UC) at 37 °C for 1 h. For N-terminal acetylation of Scc1N-GST by Naa50, 2 μg of Scc1N-GST was also added into each reaction mixture, and 70 μM non-radioactive acetyl-CoA was used in these reactions. The total volume of each reaction was 10 μl. The reactions were terminated by the addition of SDS sample buffer. Samples were resolved on SDS-PAGE followed by staining with GelCode blue reagent (Fisher). Acetylation signals were detected by exposing the dried gel to a phosphorimaging screen and analyzed with phosphorimaging. Alternatively, the reaction mixtures were blotted with the anti-Ac-Scc1N antibody.

NatA and Naa50 were purified as described (38, 41). For preparation of the Naa50-NatA complex, an excess of Naa50 was mixed with NatA, and the mixture was fractionated on a Superdex 200 gel filtration column. The fractions containing the complex were pooled. Acetyltransferase assays were performed in 25 mM HEPES, pH 7.0, 200 mM NaCl, and 1 mM DTT. The SASE and MLGP peptides used have been described previously (38, 45). In the reaction, 300 μM concentrations of radiolabeled [$^{14}$C]acetyl-CoA (4 mCi/mmol, PerkinElmer Life Sciences), 300 μM peptide, and 0.2 μM NatA, Naa50, or Naa50-NatA complex were incubated in 75 μl of total reaction volume for 1 h at 25 °C. To quench the reaction, 20 μl of the reaction mixture was added to negatively charged P81 paper (Millipore), and the paper disks were placed immediately into the wash buffer (10 mM HEPES, pH 7.5). The papers were washed 3 times (5 min per wash) to remove unreacted acetyl-CoA, dried with acetone, and then added to 4 ml of scintillation fluid. The signal was measured with a Packard Tri-Carb 1500 liquid scintillation analyzer. Reactions were performed in triplicate.

*Immunofluorescence and Chromosome Spreads*—After synchronization, mitotic cells were collected by shake-off. Cells were washed twice with PBS, incubated with 55 mM KCl at 37 °C for 15 min, and then spun onto microscope slides with a Shandon Cytospin centrifuge. Cells were extracted with the PIPES HEPES EGTA Magnesium (PHEM) buffer containing 0.3% Triton X-100 for 5 min and then fixed in 4% paraformaldehyde for 10 min. After washing three times with PBS containing 0.1% Triton X-100, the cells were incubated with the primary antibodies in PBS containing 3% BSA and 0.1% Triton X-100 at 4 °C overnight. After washing 3 times with PBS containing 0.1% Triton X-100, cells were then incubated with fluorescent secondary antibodies (Molecular Probes) in PBS containing 0.1% Triton X-100 and 3% BSA at room temperature for 1 h. Cells were again washed 3 times with PBS containing 0.1% Triton X-100 and stained with 1 μg/ml DAPI for 5 min. After the final washes, the slides were sealed with nail polish and viewed using a 100× objective on a DeltaVision fluorescence microscope (GE Healthcare). Image processing and quantification were performed with ImageJ.

For the cohesin-loading assay, cells were seeded in four-well chamber slides (LabTek). After transfection with GFP-SA2 plasmids for 7 h, cells were transfected again with the Naa50 siRNA. Cells were first extracted with PHEM buffer containing 0.5% Triton X-100 for 5 min and then fixed in 2% paraformaldehyde for 15 min. After washing with PBS, cells were blocked in PBS containing 2% BSA for 1 h and incubated with the anti-GFP and anti-tubulin antibodies in PBS containing 0.2% Triton X-100 and 3% BSA overnight at 4 °C. After washing 3 times with PBS containing 0.05% Tween 20, cells were incubated with fluorescent secondary antibodies in PBS containing 0.2% Triton X-100 and 3% BSA for 1 h at room temperature. The cells were again washed 3 times with PBS containing 0.05% Tween 20 and stained with 1 μg/ml DAPI in PBS for 5 min. After the final washes, slides were mounted and viewed with a 100× objective on a DeltaVision fluorescence microscope. Image processing and quantification were performed with ImageJ.

For chromosome spreads, mitotic cells were swelled in 55 mM KCl and fixed with methanol/acetic acid (v:v = 3:1) for 20 min at room temperature. Cells were dropped onto microscope slides, dried at room temperature, and stained with DAPI. The slides were mounted, sealed, and analyzed as described above.

*FISH*—A commercial FISH probe (BAC clone RP11-446L19 from the RPCI collection Locus 21q22.3) was ordered from Empire Genomics. Cells were fixed with methanol/acetic acid (v:v = 3:1) and dropped onto microscope slides. After being dried at room temperature, slides were treated successively with the denaturation buffer (70% formamide, 2× SSC, pH 7.0–8.0) at 73 °C and at 70%, 85%, and 100% ethanol at room temperature. Slides were dried on a warmer at 45 °C. Cells were incubated with the probe in a sealed humidified chamber with 50% formamide in 2× SSC with humidity control at 37 °C for 16 h and subsequently treated with WS1 (0.4× SSC plus 0.3% Nonidet P-40) at 73 °C and WS2 (2× SSC plus 0.1% Nonidet P-40) at room temperature. DNA was counterstained and mounted with mounting solution containing 1 μg/ml DAPI, and slides were visualized with a 100× objective on a DeltaVision fluorescence microscope. Distance measurements were performed in Image J.

*Flow Cytometry*—Cells were harvested and fixed in 70% cold ethanol overnight. After washing with PBS, cells were permeabilized with PBS containing 0.25% Triton X-100 on ice for 5 min. Then cells were incubated with the MPM2 antibody in PBS containing 1% BSA for 3 h at room temperature. After washing with PBS containing 1% BSA, cells were incubated with a fluorescent secondary antibody (Invitrogen) for 30 min. After washing with PBS, cells were resuspended in PBS containing RNase A and propidium iodide and then analyzed with a flow cytometer. Data were processed with FlowJo.

*FRAP*—HeLa Tet-On cells stably expressing human GFP-Smc1 were used in this experiment. Cells were seeded in a four-well chamber coverglass (LabTek). Expression of GFP-Smc1 was induced by the addition of 2 μg/ml doxycycline. Cells were then depleted of Naa50 by RNAi and synchronized at $G_1$/S by thymidine treatment. Cells were imaged with a 100× objective on a custom-built spinning disk confocal/total internal reflec-

tion fluorescence microscope (BioVision). An image was acquired before bleaching. A circular region in the cell nucleus was then bleached with a 405-nm laser at 100% intensity. Thirty images were then acquired at 20-s intervals after bleaching. Average intensities of GFP-Smc1 signals were measured at the bleached site with ImageJ and normalized as described (32). The half-time of recovery ($t_{1/2}$) was calculated with Prism.

*Author Contributions*—Z. R. performed most of the experiments in the paper and drafted the paper. Z. O. purified recombinant sororin and Pds5 proteins. R. S. M. designed, performed, and analyzed the experiments shown in Fig. 6. R. M. supervised and helped to analyze the experiments shown in Fig. 6. H. Y. supervised the project, analyzed the results, and wrote the paper. All authors reviewed the results, edited the manuscript, and approved the final version.

*Acknowledgments—We are grateful to Dr. Hui Zou for input at the initial stages of this study. We thank Hayden Ball for peptide synthesis, the Animal Research Center at UT Southwestern for assistance with making the acetylated Scc1 antibody, and the mass spectrometry core at UT Southwestern for mapping acetylation sites in sororin.*

**References**

1. Nasmyth, K. (2002) Segregating sister genomes: the molecular biology of chromosome separation. *Science* **297,** 559–565
2. Holland, A. J., and Cleveland, D. W. (2009) Boveri revisited: chromosomal instability, aneuploidy, and tumorigenesis. *Nat. Rev. Mol. Cell Biol.* **10,** 478–487
3. Schvartzman, J. M., Sotillo, R., and Benezra, R. (2010) Mitotic chromosomal instability and cancer: mouse modelling of the human disease. *Nat. Rev. Cancer* **10,** 102–115
4. Holland, A. J., and Cleveland, D. W. (2012) Losing balance: the origin and impact of aneuploidy in cancer. *EMBO Rep.* **13,** 501–514
5. Onn, I., Heidinger-Pauli, J. M., Guacci, V., Unal, E., and Koshland, D. E. (2008) Sister chromatid cohesion: a simple concept with a complex reality. *Annu. Rev. Cell Dev. Biol.* **24,** 105–129
6. Peters, J. M., Tedeschi, A., and Schmitz, J. (2008) The cohesin complex and its roles in chromosome biology. *Genes Dev.* **22,** 3089–3114
7. Nasmyth, K., and Haering, C. H. (2009) Cohesin: its roles and mechanisms. *Annu. Rev. Genet.* **43,** 525–558
8. Sherwood, R., Takahashi, T. S., and Jallepalli, P. V. (2010) Sister acts: coordinating DNA replication and cohesion establishment. *Genes Dev.* **24,** 2723–2731
9. Haarhuis, J. H., Elbatsh, A. M., and Rowland, B. D. (2014) Cohesin and its regulation: on the logic of X-shaped chromosomes. *Dev. Cell* **31,** 7–18
10. Ciosk, R., Shirayama, M., Shevchenko, A., Tanaka, T., Toth, A., Shevchenko, A., and Nasmyth, K. (2000) Cohesin's binding to chromosomes depends on a separate complex consisting of Scc2 and Scc4 proteins. *Mol. Cell* **5,** 243–254
11. Arumugam, P., Gruber, S., Tanaka, K., Haering, C. H., Mechtler, K., and Nasmyth, K. (2003) ATP hydrolysis is required for cohesin's association with chromosomes. *Curr. Biol.* **13,** 1941–1953
12. Watrin, E., Schleiffer, A., Tanaka, K., Eisenhaber, F., Nasmyth, K., and Peters, J. M. (2006) Human Scc4 is required for cohesin binding to chromatin, sister-chromatid cohesion, and mitotic progression. *Curr. Biol.* **16,** 863–874
13. Ladurner, R., Bhaskara, V., Huis in 't Veld, P. J., Davidson, I. F., Kreidl, E., Petzold, G., and Peters, J. M. (2014) Cohesin's ATPase activity couples cohesin loading onto DNA with Smc3 acetylation. *Curr. Biol.* **24,** 2228–2237
14. Kueng, S., Hegemann, B., Peters, B. H., Lipp, J. J., Schleiffer, A., Mechtler, K., and Peters, J. M. (2006) Wapl controls the dynamic association of cohesin with chromatin. *Cell* **127,** 955–967
15. Ouyang, Z., Zheng, G., Tomchick, D. R., Luo, X., and Yu, H. (2016) Structural basis and IP6 requirement for Pds5-dependent cohesin dynamics. *Mol. Cell* **62,** 248–259
16. Rolef Ben-Shahar, T., Heeger, S., Lehane, C., East, P., Flynn, H., Skehel, M., and Uhlmann, F. (2008) Eco1-dependent cohesin acetylation during establishment of sister chromatid cohesion. *Science* **321,** 563–566
17. Unal, E., Heidinger-Pauli, J. M., Kim, W., Guacci, V., Onn, I., Gygi, S. P., and Koshland, D. E. (2008) A molecular determinant for the establishment of sister chromatid cohesion. *Science* **321,** 566–569
18. Zhang, J., Shi, X., Li, Y., Kim, B. J., Jia, J., Huang, Z., Yang, T., Fu, X., Jung, S. Y., Wang, Y., Zhang, P., Kim, S. T., Pan, X., and Qin, J. (2008) Acetylation of Smc3 by Eco1 is required for S phase sister chromatid cohesion in both human and yeast. *Mol. Cell* **31,** 143–151
19. Rowland, B. D., Roig, M. B., Nishino, T., Kurze, A., Uluocak, P., Mishra, A., Beckouët, F., Underwood, P., Metson, J., Imre, R., Mechtler, K., Katis, V. L., and Nasmyth, K. (2009) Building sister chromatid cohesion: smc3 acetylation counteracts an antiestablishment activity. *Mol. Cell* **33,** 763–774
20. Rankin, S., Ayad, N. G., and Kirschner, M. W. (2005) Sororin, a substrate of the anaphase-promoting complex, is required for sister chromatid cohesion in vertebrates. *Mol. Cell* **18,** 185–200
21. Lafont, A. L., Song, J., and Rankin, S. (2010) Sororin cooperates with the acetyltransferase Eco2 to ensure DNA replication-dependent sister chromatid cohesion. *Proc. Natl. Acad. Sci. U.S.A.* **107,** 20364–20369
22. Nishiyama, T., Ladurner, R., Schmitz, J., Kreidl, E., Schleiffer, A., Bhaskara, V., Bando, M., Shirahige, K., Hyman, A. A., Mechtler, K., and Peters, J. M. (2010) Sororin mediates sister chromatid cohesion by antagonizing Wapl. *Cell* **143,** 737–749
23. Hauf, S., Roitinger, E., Koch, B., Dittrich, C. M., Mechtler, K., and Peters, J. M. (2005) Dissociation of cohesin from chromosome arms and loss of arm cohesion during early mitosis depends on phosphorylation of SA2. *PLos Biol.* **3,** e69
24. Gandhi, R., Gillespie, P. J., and Hirano, T. (2006) Human Wapl is a cohesin-binding protein that promotes sister-chromatid resolution in mitotic prophase. *Curr. Biol.* **16,** 2406–2417
25. Shintomi, K., and Hirano, T. (2009) Releasing cohesin from chromosome arms in early mitosis: opposing actions of Wapl-Pds5 and Sgo1. *Genes Dev.* **23,** 2224–2236
26. Dreier, M. R., Bekier, M. E., 2nd, and Taylor, W. R. (2011) Regulation of sororin by Cdk1-mediated phosphorylation. *J. Cell Sci.* **124,** 2976–2987
27. Nishiyama, T., Sykora, M. M., Huis in 't Veld, P. J., Mechtler, K., and Peters, J. M. (2013) Aurora B and Cdk1 mediate Wapl activation and release of acetylated cohesin from chromosomes by phosphorylating Sororin. *Proc. Natl. Acad. Sci. U.S.A.* **110,** 13404–13409
28. Riedel, C. G., Katis, V. L., Katou, Y., Mori, S., Itoh, T., Helmhart, W., Gálová, M., Petronczki, M., Gregan, J., Cetin, B., Mudrak, I., Ogris, E., Mechtler, K., Pelletier, L., Buchholz, F., Shirahige, K., and Nasmyth, K. (2006) Protein phosphatase 2A protects centromeric sister chromatid cohesion during meiosis I. *Nature* **441,** 53–61
29. Kitajima, T. S., Sakuno, T., Ishiguro, K., Iemura, S., Natsume, T., Kawashima, S. A., and Watanabe, Y. (2006) Shugoshin collaborates with protein phosphatase 2A to protect cohesin. *Nature* **441,** 46–52
30. Tang, Z., Shu, H., Qi, W., Mahmood, N. A., Mumby, M. C., and Yu, H. (2006) PP2A is required for centromeric localization of Sgo1 and proper chromosome segregation. *Dev. Cell* **10,** 575–585
31. Liu, H., Jia, L., and Yu, H. (2013) Phospho-H2A and cohesin specify distinct tension-regulated Sgo1 pools at kinetochores and inner centromeres. *Curr. Biol.* **23,** 1927–1933
32. Liu, H., Qu, Q., Warrington, R., Rice, A., Cheng, N., and Yu, H. (2015) Mitotic transcription installs Sgo1 at centromeres to coordinate chromosome segregation. *Mol. Cell* **59,** 426–436
33. Liu, H., Rankin, S., and Yu, H. (2013) Phosphorylation-enabled binding of SGO1-PP2A to cohesin protects sororin and centromeric cohesion during mitosis. *Nat. Cell Biol.* **15,** 40–49
34. Starheim, K. K., Gevaert, K., and Arnesen, T. (2012) Protein N-terminal acetyltransferases: when the start matters. *Trends Biochem. Sci.* **37,** 152–161
35. Williams, B. C., Garrett-Engele, C. M., Li, Z., Williams, E. V., Rosenman, E. D., and Goldberg, M. L. (2003) Two putative acetyltransferases, san and

deco, are required for establishing sister chromatid cohesion in *Drosophila*. *Curr. Biol.* **13,** 2025–2036
36. Hou, F., Chu, C. W., Kong, X., Yokomori, K., and Zou, H. (2007) The acetyltransferase activity of San stabilizes the mitotic cohesin at the centromeres in a shugoshin-independent manner. *J. Cell Biol.* **177,** 587–597
37. Gautschi, M., Just, S., Mun, A., Ross, S., Rücknagel, P., Dubaquié, Y., Ehrenhofer-Murray, A., and Rospert, S. (2003) The yeast *N*(α)-acetyltransferase NatA is quantitatively anchored to the ribosome and interacts with nascent polypeptides. *Mol. Cell. Biol.* **23,** 7403–7414
38. Liszczak, G., Arnesen, T., and Marmorstein, R. (2011) Structure of a ternary Naa50p (NAT5/SAN) N-terminal acetyltransferase complex reveals the molecular basis for substrate-specific acetylation. *J. Biol. Chem.* **286,** 37002–37010
39. Evjenth, R., Hole, K., Karlsen, O. A., Ziegler, M., Arnesen, T., and Lillehaug, J. R. (2009) Human Naa50p (Nat5/San) displays both protein Nα- and Nϵ-acetyltransferase activity. *J. Biol. Chem.* **284,** 31122–31129
40. Chu, C. W., Hou, F., Zhang, J., Phu, L., Loktev, A. V., Kirkpatrick, D. S., Jackson, P. K., Zhao, Y., and Zou, H. (2011) A novel acetylation of β-tubulin by San modulates microtubule polymerization via down-regulating tubulin incorporation. *Mol. Biol. Cell* **22,** 448–456
41. Magin, R. S., March, Z. M., and Marmorstein, R. (2016) The N-terminal acetyltransferase Naa10/ARD1 does not acetylate lysine residues. *J. Biol. Chem.* **291,** 5270–5277
42. Ouyang, Z., Zheng, G., Song, J., Borek, D. M., Otwinowski, Z., Brautigam, C. A., Tomchick, D. R., Rankin, S., and Yu, H. (2013) Structure of the human cohesin inhibitor Wapl. *Proc. Natl. Acad. Sci. U.S.A.* **110,** 11355–11360
43. Hara, K., Zheng, G., Qu, Q., Liu, H., Ouyang, Z., Chen, Z., Tomchick, D. R., and Yu, H. (2014) Structure of cohesin subcomplex pinpoints direct shugoshin-Wapl antagonism in centromeric cohesion. *Nat. Struct. Mol. Biol.* **21,** 864–870
44. Van Damme, P., Evjenth, R., Foyn, H., Demeyer, K., De Bock, P. J., Lillehaug, J. R., Vandekerckhove, J., Arnesen, T., and Gevaert, K. (2011) Proteome-derived peptide libraries allow detailed analysis of the substrate specificities of *N*(α)-acetyltransferases and point to hNaa10p as the post-translational actin *N*(α)-acetyltransferase. *Mol. Cell Proteomics* 10.1074/mcp.M110.004580
45. Liszczak, G., Goldberg, J. M., Foyn, H., Petersson, E. J., Arnesen, T., and Marmorstein, R. (2013) Molecular basis for N-terminal acetylation by the heterodimeric NatA complex. *Nat. Struct. Mol. Biol.* **20,** 1098–1105
46. Yi, C. H., Pan, H., Seebacher, J., Jang, I. H., Hyberts, S. G., Heffron, G. J., Vander Heiden, M. G., Yang, R., Li, F., Locasale, J. W., Sharfi, H., Zhai, B., Rodriguez-Mias, R., Luithardt, H., Cantley, L. C., Daley, G. Q., Asara, J. M., Gygi, S. P., Wagner, G., Liu, C. F., and Yuan, J. (2011) Metabolic regulation of protein *N*-α-acetylation by Bcl-xL promotes cell survival. *Cell* **146,** 607–620
47. Scott, D. C., Monda, J. K., Bennett, E. J., Harper, J. W., and Schulman, B. A. (2011) N-terminal acetylation acts as an avidity enhancer within an interconnected multiprotein complex. *Science* **334,** 674–678
48. Van Damme, P., Hole, K., Gevaert, K., and Arnesen, T. (2015) N-terminal acetylome analysis reveals the specificity of Naa50 (Nat5) and suggests a kinetic competition between N-terminal acetyltransferases and methionine aminopeptidases. *Proteomics* **15,** 2436–2446
49. Mǹdez, J., and Stillman, B. (2000) Chromatin association of human origin recognition complex, Cdc6, and minichromosome maintenance proteins during the cell cycle: assembly of prereplication complexes in late mitosis. *Mol. Cell. Biol.* **20,** 8602–8612